## AD NUMBER

**AD001911**

## NEW LIMITATION CHANGE

TO

**Approved for public release, distribution unlimited**

FROM

**Distribution: No Foreign.**

## AUTHORITY

**ONR ltr., 26 Oct 1977**

REPORT NO. HE-150-106

TECHNICAL REPORT

UNIVERSITY OF CALIFORNIA

INSTITUTE OF ENGINEERING RESEARCH

BERKELEY CALIFORNIA

# HEAT TRANSFER FROM SPHERES TO A RAREFIED GAS IN SUBSONIC FLOW

By

L. L. KAVANAU and R. M. DRAKE, JR.

SERIES NO. 20

ISSUE NO. 94

DATE JANUARY 23, 1953

CONTRACT N7-ONR-295-TASK 3
PROJECT NR 061-003
REPORT NO. HE-150-108
SERIES NO. 20-94
JANUARY 23, 1953

JOINTLY SPONSORED BY
OFFICE OF NAVAL RESEARCH AND
OFFICE OF SCIENTIFIC RESEARCH

# FLUID FLOW AND HEAT TRANSFER AT LOW PRESSURES AND TEMPERATURES

## HEAT TRANSFER FROM SPHERES TO A RAREFIED GAS IN SUBSONIC FLOW

By

L. L. KAVANAU and R. M. DRAKE, JR.

FACULTY INVESTIGATORS:

R. G. FOLSOM, PROFESSOR OF MECHANICAL ENGINEERING

S. A. SCHAAF, ASSOCIATE PROFESSOR OF ENGINEERING SCIENCES

Approved by: S A Schaaf

## NOMENCLATURE

$A$ = surface area of sphere, sq. ft.

$a$ = speed of sound, ft/sec

$c, c_p$ = specific heat, BTU/lb°F

$D$ = sphere diameter, ft.

$h$ = heat transfer convection coefficient, BTU/hr $ft^2$°F

$h_c$ = average overall convection coefficient, BTU/hr $ft^2$°F

$h_r$ = average overall radiation coefficient, BTU/hr $ft^2$°F

$J_1, Y_1$ = Bessel functions of the first kind, order 1

$k$ = thermal conductivity, BTU/hr ft°F

$\lambda$ = molecular mean free path, ft.

$M$ = Mach number $\left(\frac{U}{a}\right)$, dimensionless

$n$ = $\frac{U_x}{U_{av}}$, dimensionless

$Nu$ = Nusselts number $\left(\frac{hx}{k}\right)$, dimensionless

$Nu_{av}$ = average Nusselts number $\left(\frac{h_{av}D}{k}\right)$, dimensionless

$p_i$ = impact pressure on probe, microns of Hg.

$p_s$ = nozzle wall static pressure, microns of Hg.

$Pr$ = Prandtl number $\left(\frac{\mu c_p}{k} = 0.72 \text{ for air}\right)$, dimensionless

$q$ = heat flux, BTU/hr $ft^2$

$Re$ = Reynolds number $\left(\frac{U\rho x}{\mu}\right)$, dimensionless

$Re_1$ = free stream Reynolds number $\left(\frac{U_1\rho_1 D}{\mu_1}\right)$, dimensionless

$Re_2$ = free stream Reynolds number behind normal shock wave in supersonic flow $\left(\frac{U_2\rho_2 D}{\mu_2}\right)$, identical to $Re_1$ for subsonic flow, dimensionless

$t$ = temperature, °F

$t_e$ = surface equilibrium temperature due to convection, °F

$t_e'$ = surface equilibrium temperature due to convection, radiation, and conduction, °F

$t_a$ = tunnel wall temperature, °F

$t_i$ = initial temperature of sphere, °F

$T$ = absolute temperature, °R

$U$ = velocity, ft/sec

$V$ = volume of sphere, $ft^3$

$u$ = arbitrary variable of integration

$w$ = specific weight of sphere, $lbs/ft^3$

$x$ = characteristic length, ft.

$y$ = distance along outward normal from surface, ft.

$\alpha$ = thermal accommodation coefficient, dimensionless

$\beta$ = parameter $\sqrt{\frac{2}{\pi} Re Pr}$, dimensionless

$\gamma$ = ratio of specific heats, dimensionless

$\theta$ = parameter, $1.996 \frac{2-\alpha}{\alpha} \cdot \frac{\gamma}{\gamma+1}$, dimensionless

$\lambda$ = temperature jump distance $\left(\frac{\theta l}{Pr}\right)$, ft.

$\mu$ = absolute viscosity, lbs sec/$ft^2$

$\rho$ = mass density, lbs $sec^2/ft^4$

$\tau$ = time, hr.

SUBSCRIPTS:

$0$ = stagnation conditions

$1$ = free stream conditions

$2$ = stream conditions behind normal shock wave in supersonic flow

$av$ = an integrated average

$e$ = surface equilibrium conditions

$w$ = surface conditions

$y=0$ = stream conditions adjacent to the surface

SUPERSCRIPTS:

$o$ = continuum conditions

# HEAT TRANSFER FROM SPHERES TO A RAREFIED GAS IN SUBSONIC FLOW

## 1.0 INTRODUCTION

Convective heat transfer from spheres to a rarefied gas has been treated analytically and experimentally in Refs. 1, 2, 3 and 4. From the experimental results of Ref. 4, the predicted effect of gas rarefaction on the heat transfer in the slip flow region was in part substantiated, in that the heat transfer coefficient decreased below its continuum value, with increasing rarefaction. This effect is apparently (Ref. 1) primarily due to the temperature jump condition at the surface, analogous to the slip velocity at the surface, which occurs at low pressures. This temperature jump introduces an effective thermal contact resistance at the surface.

The experimental results of Ref. 4 were determined under supersonic flow conditions. Since there existed a curved detached shock wave, some doubt remained as to the effect of the shock wave and possibly other compressibility phenomena on the results. It was considered desirable to obtain heat transfer data from spheres at subsonic Mach numbers in the slip flow region.

It is the purpose of this report to present overall average heat transfer data from spheres to a rarefied air stream for a range of variables, $0.1 \leq M \leq 0.69$ and $1.7 \leq Re \leq 124$, and to present a simplified analysis which predicts the trends of this data by a rarefaction correction to the continuum solution. An expression for the non-dimensional overall average heat transfer coefficient for spheres in subsonic flow is obtained in the form

$$Nu_{av} = \frac{Nu_{av}^{\circ}}{1 + 3.42 \frac{M_1}{Re_1 Pr} Nu_{av}^{\circ}}$$

The flow regions investigated here and in Ref. 4 are shown on Fig. 1 in comparison with the range of earlier investigations reported in Ref. 5.

## 2.0 ANALYSIS

If one considers the temperature jump in the slip flow region as an effective thermal contact resistance at the surface over and above

the thermal resistance due to the viscous boundary layer, then the heat transfer coefficient at low pressures can be determined to the first order by a correction to the continuum heat transfer coefficient at the same Reynolds number.

Consider a surface placed in a continuum flow so that heat is transfered between the surface and the stream. At any particular instant the surface temperature is assumed uniform and equal to $t_w^\circ$. The heat flux will be

$$q = -k_{y=o} \left.\frac{\partial t}{\partial y}\right)_{y=o} = h_c^\circ \left(t_w^\circ - t_e^\circ\right) \tag{2.1}$$

where $\frac{\partial t}{\partial y}$ is the gradient of temperature normal to the surface, $K$ is the heat conductivity, $h_c$ is the convective heat transfer coefficient, and $t_e$ is the equilibrium temperature of the surface. The subscript $y = o$ identifies the properties of the air evaluated at the surface and zero superscript signifies continuum conditions.

Now if the air stream is rarefied while holding the Reynolds number constant, the additional resistance to heat transfer due to the temperature jump will present itself so that we may define a total convective heat transfer coefficient incorporating both the thermal boundary layer and temperature jump resistances by writing

$$q = h_c \left(t_w - t_e\right) \tag{2.2}$$

where $t_w$ and $t_e$ are the surface temperature and equilibrium surface temperature respectively.

The first order temperature jump boundary condition may be written as

$$t_{y=o} - t_w = \lambda \left.\frac{\partial t}{\partial y}\right)_{y=o} \tag{2.3}$$

where $t_{y=o}$ and $\left.\frac{\partial t}{\partial y}\right)_{y=o}$ are the temperature and gradient of temperature in the layer of gas immediately adjacent to the surface. The quantity $\lambda$ is the temperature jump distance defined from kinetic theory (Ref. 6) by the formula

$$\lambda = 1.996 \frac{2-\alpha}{\alpha} \frac{\gamma}{\gamma+1} \frac{\ell}{Pr}$$

or:

$$\lambda = \frac{\Theta}{Pr} \ell \tag{2.4}$$

with $\lambda = 1.48 \frac{\alpha M}{Re}$, $\alpha$ the accommodation coefficient, $\gamma$ the ratio of specific heats, $Pr$ the Prandtl number, and $\Theta = 1.996 \frac{2-\alpha}{\alpha} \frac{\gamma}{\gamma+1}$.

This first order temperature jump condition requires that $t_e = t_e^\circ$. It is now further assumed that $q$, the heat transfered between the sphere at temperature $t_w$ and the gas at temperature $t_1$ for the case of a surface temperature jump, is the same as the heat transfered between a sphere at temperature $t_{y=o}$ and the gas at temperature $t_1$ under conditions of no temperature jump. In other words, Eq. 2.1 is assumed valid with $t_w^\circ = t_{y=o}$.

Combinations of Eqs. 2.1, 2.2 and 2.3 give

$$\frac{h_c^\circ}{h_c} = 1 + \frac{\lambda h_c^\circ}{k_{y=o}} \tag{2.5}$$

Substituting Eq. 2.4 in 2.5 yields

$$\frac{h_c^\circ}{h_c} = 1 + 1.48\,\Theta\,\frac{h_c^\circ x}{k_{y=o}} \cdot \frac{M}{Re\,Pr} \tag{2.6}$$

or

$$\frac{Nu^\circ}{Nu} = 1 + 1.48\,\Theta\,\frac{M}{Re\,Pr}\,Nu^\circ \tag{2.7}$$

where $Nu^\circ$ and $Nu$ are the local Nusselts numbers for continuum and rarefied flows respectively.

Eq. 2.7 indicates that experimental data could be correlated by a plot of $\left(\frac{1}{Nu} - \frac{1}{Nu^\circ}\right)$ versus $\frac{M}{Re\,Pr}$, see Fig. 4.

## 3.0 EXPERIMENTAL EQUIPMENT AND PROCEDURE

3.1 The required low density gas stream was provided by the No. 3 Wind Tunnel located at Berkeley. The constructional features and general operating characteristics of the tunnel are contained in Ref. 7. An axi-symmetric, subsonic nozzle was employed in the investigation, giving a range of Mach numbers, 0.1 to 0.69, and a static pressure range of 36 to 3300 microns Hg. The nozzle used had an exit diameter of 9 inches. The design of this nozzle is described in Ref. 8.

The four spheres and the impact pressure probe were mounted on a rotary selector (see Appendix C, Ref. 8) which in turn was supported

in the tunnel test chamber by a traversing mechanism (Ref. 7) capable of axial, lateral, and vertical movement with respect to the nozzle. With this versatile mounting system, any of the five objects on the rotary selector could be moved into the flow field as required, without alteration of the flow.

3.2 Experimental Method

The overall average heat transfer coefficients were determined by the transient technique described in Ref. 4. Briefly, the method is as follows: The rate of change of heat in a small body of sensibly uniform internal temperature distribution is equated to the heat loss by convection and radiation to give

$$-cwV\frac{dt}{d\tau} = h_c A (t - t_e) + h_r A (t - t_a) \tag{3.1}$$

with the boundary conditions

$$t = t_i \qquad \tau = 0$$

$$t = t_e' \qquad \tau \to \infty$$

where $t_i$ is the initial sphere temperature and $t_e'$ is the equilibrium temperature for the combined effects of radiation and convection. If the difference between the absolute surface temperature and the absolute temperature of the surroundings is not great, Eq. 3.1 may be integrated for $h_c$ and $h_r$ not functions of the temperature to yield,

$$\frac{t - t_e'}{t_i - t_e'} = e^{-\frac{A(h_c + h_r)}{cwV}\tau} \tag{3.2}$$

where the equilibrium temperature $t_e'$ is,

$$t_e' = \frac{h_c t_e + h_r t_a}{(h_c + h_r)} \tag{3.3}$$

and the equilibrium temperature due to convection heat transfer alone is given from Eq. 3.3 as

$$t_e = t_e' + \frac{h_r}{h_c}(t_e' - t_a) \tag{3.4}$$

It is necessary to determine the radiation heat transfer coefficient $h_r$ independently by making transient cooling runs at no flow

with tunnel pressures reduced to the order of 0.1 mm Hg, so that free convection currents are eliminated. The heat balance in this case becomes

$$-cwV\frac{dt}{d\tau} = h_r A (t - t_a) \tag{3.5}$$

and the solution for the boundary condition

$$t = t_i \qquad \tau = 0$$
$$t = t_a \qquad \tau \to \infty$$

$$\frac{t - t_a}{t_i - t_a} = e^{-\frac{Ah_r \tau}{cwV}} \tag{3.6}$$

Making use of the temperature time histories on a semi-logarithmic plot as suggested by Eqs. 3.2 and 3.6, the radiation heat transfer coefficient, $h_r$, and the sum of the radiation and convection coefficients $(h_c + h_r)$ are obtained. The quantity $t_a$ is measured by means of a thermocouple placed on the tunnel wall and $t_e'$ is that equilibrium temperature attained by the sphere after a very long time. The equilibrium temperature for convection only may then be calculated from Eq. 3.4. The heat transfer coefficient due to convection alone, $h_c$, is the arithmetic difference between the two experimentally determined coefficients $(h_c+h_r)$ and $h_r$.

## 3.3 Spheres

The spheres were made of silver and were mounted on hollow drawn glass stings as shown in Fig. 2. B and S No. 40 iron and constantan wires were made into thermocouples and soft soldered into the centers of the spheres and were then led out through the glass stings to larger wires on the sting support leading to the recording potentiometer. The spheres are further described in Ref. 4.

## 3.4 Experimental Procedure

The sphere in question was heated initially to a temperature of approximately 120°-150°F by means of a radiation furnace consisting of a 100 watt lamp encased in several radiation shields and mounted near the nozzle in the test chamber. This radiant energy was sufficient to give the sphere a 10° temperature rise in approximately 10 seconds. The sphere was then removed from the furnace and traversed

into the air stream on the nozzle centerline with its forward stagnation point tangent to the exit plane of the nozzle. The temperature-time history of the sphere for this position was recorded by means of the recording potentiometer.

### 3.5 Instrumentation

All pressures were measured by a precision U-tube manometer (Ref. 9) to an accuracy of $\pm$ 1 microns Hg for pressures up to 400 microns and $\pm$ 1/4 per cent for pressures above 400 microns.

Sphere temperatures were measured by an iron-constantan thermocouple and recorded by a Leeds-Northrup potentiometer to an accuracy of $\pm$ .017 millivolts $\pm$ 0.5°F and 2.5 per cent in time. The tunnel wall temperature, $T_a$ , and settling chamber temperature, $T_o$ , were measured by copper-constantan thermocouples located in the settling chamber and recorded with a Brown 16 point recording potentiometer to $\pm$ .03 millivolts ($\pm$ 1.4°F).

In addition to the above special instrumentation, the standard tunnel equipment and instrumentation as described in Ref. 7 was utilized.

## 4.0 REDUCTION OF EXPERIMENTAL DATA

### 4.1 Flow System

The flow parameters required in the data presentation are Mach number and Reynolds numbers evaluated at the center of the nozzle exit plane. These values were determined in the following manner: The static pressure, $p_s$ , was measured by a wall orifice in the constant area section of the nozzle and the total or impact pressure $p_i$ was measured by a source-shaped impact probe (0.300" O.D.) at the nozzle exit plane. Agreement between this impact pressure and the reservoir pressure allowed the use of the following isentropic formula for the determination of Mach number:

$$\frac{p_i}{p_s} = \left(1 + \frac{\gamma-1}{2} M_1^2\right)^{\frac{\gamma}{\gamma-1}} \tag{4.1}$$

for air with $\gamma = 1.4$

$$M_1 = 2.236 \left[\left(\frac{p_i}{p_s}\right)^{.286} - 1\right]^{\frac{1}{2}} \tag{4.2}$$

The stagnation temperature was assumed identical to the measured settling chamber temperature. As a result, the state temperature was determined from the Mach number by the adiabatic formula

$$T_1 = T_0 \left(1 + \frac{\gamma-1}{2} M_1^2\right)^{-1} \tag{4.3}$$

and for $\gamma = 1.4$

$$T_1 = T_0 \left(1 + 0.2 M_1^2\right)^{-1} \tag{4.4}$$

Assuming that perfect gas relationship holds, the above formulas for $M_1$ and $T_1$, together with the measured value of $p_s$ and the coefficient of viscosity for dry air at temperature $T_1$ (Ref. 10) enabled the Reynolds number to be calculated by the formula

$$Re_1 = 6.64 \times 10^{-6} \frac{M_1 p_s D}{\mu_1 \sqrt{T_1}} \tag{4.5}$$

In Table I are tabulated the tunnel flow conditions for the various runs. No nozzle blocking corrections were applied.

## 4.2 Thermal System

The reduction of the thermal data was accomplished by means of the method outlined in Section 3.2 to result in the values of the convection coefficients $h_c$. The final results are shown in Table II in the dimensionless form of the Nusselts number, $Nu_{av} = \frac{h_c D}{k_e}$, wherein the thermal conductivity of the air is evaluated at the equilibrium temperature of the sphere. A typical plot of $\log(T - T_e)$ versus $\tau$ appears in Fig. 3.

# 5.0 SOURCES OF ERROR

## 5.1 Flow System

Errors incurred in the determination of the Mach and Reynolds numbers were primarily due to the inaccuracy of the instrumentation used to measure the pressures and temperature required in Eqs. 4.2 and 4.5. The maximum relative errors of these quantities vary from 0.1 to 25 per cent and are listed with the quantities themselves in Table I.

## 5.2 Thermal System

The errors attendant to the determination of the heat transfer

coefficients $h_c$ reside in the measurement of the time-temperature history of the cooling body and in the separate determination of the equilibrium temperature $t_e'$. These errors are thus determined by the least count of the recording potentiometers. The largest least count, $\pm$ .52°F, when associated with the smallest temperature difference measured and used in the computation, 5°F, gives a possible error of 10 per cent. In addition, the error due to time measurement is 2.5 per cent. The radiation-conduction correction which is accounted for experimentally in independent runs is subject to the same errors due to instrumentation. Since the radiation-conduction correction may amount to 50 per cent of the total heat transfer coefficient $(h_c + h_r)$ in the worst case, the maximum uncertainty in the determination of $h_c$ may possibly be 25 per cent. This uncertainty in $h_c$ will be transmitted directly to the Nusselts number with any other error incurred in the value of the thermal conductivity of the air.

## 6.0 DISCUSSION OF EXPERIMENTAL RESULTS

The analysis given in Section 2.0 results in an expression for the dimensionless local heat transfer coefficient for the case of slip flow by virtue of an effective thermal contact resistance due to the temperature jump boundary condition. The result appears as a function of the dimensionless local heat transfer coefficient for continuum flow and the local Mach, Reynolds and Prandtl numbers. It is given as

$$Nu = \frac{Nu^o}{1 + 1.48\,\theta \frac{M}{Re\,Pr} Nu^o} \tag{6.1A}$$

or

$$\left(\frac{1}{Nu} - \frac{1}{Nu^o}\right) = 1.48\,\theta\,\frac{M}{Re\,Pr} \tag{6.1B}$$

The experimental data is in the form of overall average heat transfer coefficients on spheres and exact prediction of these results cannot be expected from the foregoing simplified analysis. However, one could expect that Eq. 6.1A would give a method of correlating the data, insofar as it reduces to the continuum value for small $\frac{M}{Re\,Pr}$ and gives a solution for large $\frac{M}{Re\,Pr}$ which resembles the free molecule solution of Ref. 3, i.e., $\frac{Nu}{Re\,Pr} = \frac{f(\gamma, \alpha)}{M}$, for small M.

For our particular application to overall average heat transfer from spheres, we shall utilize the solution from Ref. 2 as the specification for $Nu^{\circ}$ which gives

$$Nu_{av}^{\circ} = \left(\frac{h_{av} D}{k}\right)^{\circ} = 2 + \frac{2}{\pi^2} \int_0^{\infty} \frac{\left(1 - e^{-u^2 \pi}\right)\left(1 + u^4\right)^{-1}}{J_1^2(\beta, u) + Y_1^2(\beta, u)} \cdot \frac{du}{u} \qquad (6.2)$$

where $\beta = \sqrt{\frac{2}{n} Re\, Pr}$ , $n = \frac{U_1}{U_{av}}$ with $U_1$ the free stream velocity and $U_{av}$ the average velocity over the sphere. The experimental data is correlated as $\frac{1}{Nu_{av}} - \frac{1}{Nu_{av}^{\circ}}$ versus $\frac{M}{Re\, Pr}$ and appears in Fig. 4 with $n = 1.3$. The value of $n = 1.3$ was chosen merely to match the solution to the data for small $\frac{M}{Re\, Pr}$ . The data correlates as a straight line of slope equal to 3.42 as determined by the method of least squares. It may be seen in Fig. 4 that better than 90 per cent of all the experimental data lies within a 10 per cent error by $Nu_{av}$ of this line. This is, in general, within the accuracy of measurement of the data.

The above empirically determined constant, 3.42, enables one to write an expression for the heat transfer for spheres in a slightly rarefied subsonic air stream as

$$Nu_{av} = \frac{Nu_{av}^{\circ}}{1 + 3.42 \frac{M_1}{Re_1 Pr} Nu_{av}^{\circ}} \qquad (6.3)$$

The superimposed plot of Eq. 6.3 as well as the theoretical results for spheres from Refs. 2 and 3 are shown for comparison with the experimental data in Fig. 5 as Nusselts number versus Reynolds number with Mach number as the parameter. This figure presents graphically the growing influence of the rarefaction parameter $\frac{M}{Re}$ upon the heat transfer and also illustrates the ability of the proposed rarefaction correction to match the continuum and free molecule flow solutions.

In Fig. 6 analytical results of the continuum low Reynolds number and free molecule flow regions are shown for comparison with known existing experimental data for heat transfer from spheres.

Temperature recovery factors have not been presented because the instrumentation used prevented obtaining an acceptable accuracy in the measurement of this quantity.

## 7.0 RESULTS

7.1 Experimental average overall heat transfer coefficients were obtained for spheres in a rarefied subsonic air stream where the Mach number and Reynolds number varied from 0.1 to 0.69 and 1.7 to 124, respectively.

7.2 A semi-empirical formulation of the Nusselts number for spheres in a rarefied subsonic air stream is obtained by correcting the continuum solution for an effective thermal contact resistance due to the temperature jump boundary condition.

7.3 The presented data follow the same trends toward the free molecule solution as was first shown in Ref. 4 for spheres in rarefied supersonic flows.

## 8.0 REFERENCES


1) R. M. Drake, Jr. and E. D. Kane - "Heat Transfer Problems in High Speed Flows in Rarefied Gases", General Discussion of Heat Transfer, London, Sept. 1951 - also Univ. of Calif. Eng. Projects Report HE-150-73, Oct. 1950

2) R. M. Drake, Jr., F. M. Sauer and S. A. Schaaf - "Forced Convection Heat Transfer from Cylinders and Spheres in a Rarefied Gas", Univ. of Calif. Eng. Projects Report HE-150-74, Nov. 1950

3) F. M. Sauer - "Convective Heat Transfer from Spheres in a Free Molecule Flow", Jour. Aero. Sci., Vol. 18, No. 5, May 1951, pp 353-354 - also Univ. of Calif. Eng. Projects Report HE-150-77, Jan. 1951

4) R. M. Drake, Jr. and G. H. Backer - "Heat Transfer from Spheres to a Rarefied Gas in Supersonic Flow", Trans. Amer. Soc. Mech. Engrs., Vol. 74, No. 7, Oct. 1952 - also Univ. of Calif. Eng. Projects Report HE-150-78, Feb. 1951

5) W. H. McAdams - "Heat Transmission", McGraw-Hill Book Co., 1942

6) E. H. Kennard - "Kinetic Theory of Gases", McGraw-Hill Book Co., 1938

7) S. A. Schaaf, D. O. Horning and E. D. Kane - "Design and Initial Operation of a Low Density Supersonic Wind Tunnel", Trans. of Heat Transfer & Fluid Mechanics Institute, ASME, June 1949 - also Univ. of Calif. Eng. Projects Report HE-150-62, Aug. 1949

8) F. S. Sherman - "New Experiments on Impact Pressure Interpretation in Supersonic and Subsonic Airstreams", Univ. of Calif. Eng. Projects Report HE-150-99, Dec. 1951

9) G. J. Maslach - "A Precision Manometer for Low Pressures", Rev. Sci. Instruments, Vol. 23, No. 7, pp 367-369, July 1952 - also Univ. of Calif. Eng. Projects Report HE-150-75, Oct. 1950

10) - The NBS-NACA Tables of Thermal Properties of Dry Air, Dec. 1950

11) H. W. Emmons - "Gas Dynamics Tables for Air", Dover Publications, Inc., New York, 1947

TABLE I

SUBSONIC NOZZLE FLOW CONDITIONS

| Tunnel Run No. | Flow Rate (lbs/hr) | $p_s$ (microns Hg) | $T_o$ (°R) | M | Re (per inch) | Maximum Error (per cent) | |
|---|---|---|---|---|---|---|---|
| | | | | | | M | Re |
| 236(a) | 20 | 193 | 538 | .69 | 110 | ± .1 | ± .6 |
| 236(b) | 20 | 374 | 539 | .37 | 116 | ± 1.3 | ± 1.6 |
| 237 | 20 | 363 | 535 | .37 | 106 | ± 1.3 | ± 1.6 |
| 238 | 2.3 | 36 | 543 | .59 | 17 | ± 5.7 | ± 8.5 |
| 239 | 2.3 | 136 | 537 | .17 | 17 | ±17 | ±17 |
| 240 | 2.3 | 63 | 543 | .35 | 17 | ± 7.7 | ± 9.3 |
| 241 | 2.3 | 62 | 538 | .37 | 18 | ± 7.7 | ± 9.3 |
| 242(a) | 2.3 | 61 | 536 | .37 | 18 | ± 7.7 | ± 9.3 |
| 242(b) | 2.3 | 241 | 536 | .10 | 18 | ±25 | ±25 |
| 243 | 2.3 | 236 | 538 | .10 | 17 | ±25 | ±25 |
| 244 | 50 | 3293 | 539 | .10 | 248 | ±16 | ±16 |
| 245 | 40 | 1305 | 543 | .21 | 205 | ± 3.6 | ± 3.9 |
| 246(a) | 40 | 738 | 538 | .37 | 207 | ± 1.2 | ± 1.5 |
| 246(b) | 40 | 440 | 543 | .59 | 211 | ± .5 | ± .8 |
| 247 | 30 | 570 | 530 | .37 | 166 | ± 1.2 | ± 1.5 |

TABLE II

| Tunnel Run No. | Sphere Diameter (inches) | $h_{r+c}$ | $t_e$ (°F) | $h_r$ | $h_c$ | $Nu_{av}$ | $Re_l$ | $M_l$ |
|---|---|---|---|---|---|---|---|---|
| 236(a) | .100 | 4.00 | 72.5 | .84 | 3.16 | 1.76 | 11.0 | .69 |
| | .175 | 2.50 | 70.1 | .54 | 1.96 | 1.92 | 19.3 | .69 |
| | .250 | 2.31 | 68.9 | .23 | 2.08 | 2.91 | 27.6 | .69 |
| | .500 | 1.53 | 69.4 | .12 | 1.41 | 3.95 | 55.1 | .69 |
| 236(b) | .100 | 4.91 | 77.6 | .84 | 4.06 | 2.24 | 11.6 | .37 |
| | .250 | 2.66 | 77.5 | .23 | 2.43 | 3.36 | 29.1 | .37 |
| 237 | .175 | 3.22 | 77.8 | .54 | 2.68 | 2.59 | 18.5 | .37 |
| 238 | .100 | 1.72 | 83.9 | .84 | .844 | .477 | 1.69 | .59 |
| | .175 | .98 | 83.1 | .28 | .703 | .673 | 2.96 | .59 |
| | .250 | 1.07 | 81.1 | .23 | .834 | 1.14 | 4.23 | .59 |
| | .500 | .71 | 78.2 | .12 | .59 | 1.63 | 8.46 | .59 |
| 239 | .100 | 3.01 | 78.5 | .84 | 2.17 | 1.19 | 1.73 | .17 |
| | .175 | 1.80 | 78.3 | .28 | 1.52 | 1.47 | 3.03 | .17 |
| | .250 | 1.58 | 78.4 | .23 | 1.35 | 1.86 | 4.32 | .17 |
| | .500 | 1.06 | 78.2 | .12 | .94 | 2.58 | 8.66 | .17 |
| 240 | .500 | .81 | 73.7 | .12 | .69 | 1.90 | 8.37 | .35 |
| 241 | .175 | 1.31 | 78.6 | .28 | 1.03 | .99 | 3.14 | .37 |
| | .250 | 1.26 | 77.9 | .23 | 1.03 | 1.42 | 4.49 | .37 |
| 242(a) | .100 | 2.19 | 73.2 | .84 | 1.35 | .75 | 1.76 | .37 |
| 242(b) | .500 | 1.05 | 73.0 | .12 | .93 | 2.58 | 8.75 | .10 |
| 243 | .100 | 3.62 | 76.6 | .84 | 2.78 | 1.54 | 1.73 | .10 |
| | .175 | 2.12 | 77.6 | .28 | 1.84 | 1.78 | 3.02 | .10 |
| | .250 | 1.97 | 76.3 | .23 | 1.73 | 2.40 | 4.33 | .10 |
| 244 | .100 | 7.92 | 75.3 | .84 | 7.08 | 3.92 | 24.8 | .10 |
| | .175 | 4.92 | 75.3 | .28 | 4.64 | 4.50 | 43.3 | .10 |
| | .250 | 4.06 | 76.2 | .23 | 3.83 | 5.30 | 61.9 | .10 |
| | .500 | 2.60 | 76.3 | .12 | 2.48 | 6.86 | 124.0 | .10 |
| 245 | .100 | 7.10 | 79.6 | .84 | 6.26 | 3.45 | 20.5 | .21 |
| | .175 | 4.40 | 79.6 | .28 | 4.12 | 3.97 | 35.2 | .21 |
| | .250 | 3.82 | 79.6 | .23 | 3.59 | 4.94 | 50.3 | .21 |
| | .500 | 2.57 | 78.7 | .12 | 2.45 | 6.75 | 101.0 | .21 |
| 246(a) | .100 | 6.60 | 68.6 | .84 | 5.76 | 3.23 | 20.8 | .37 |
| | .175 | 4.13 | 69.1 | .28 | 3.85 | 3.77 | 36.3 | .37 |
| | .250 | 3.56 | 70.7 | .23 | 3.33 | 4.65 | 51.9 | .37 |
| | .500 | 2.39 | 71.2 | .12 | 2.27 | 6.33 | 103.0 | .37 |
| 246(b) | .100 | 5.95 | 69.5 | .84 | 5.11 | 2.86 | 27.1 | .59 |
| | .175 | 3.70 | 69.5 | .28 | 3.42 | 3.35 | 36.8 | .59 |
| | .250 | 3.26 | 70.8 | .23 | 3.03 | 4.22 | 52.6 | .59 |
| | .500 | 2.22 | 68.4 | .12 | 2.09 | 5.87 | 105.0 | .59 |
| 247 | .100 | 5.89 | 69.5 | .84 | 4.95 | 2.77 | 16.6 | .37 |

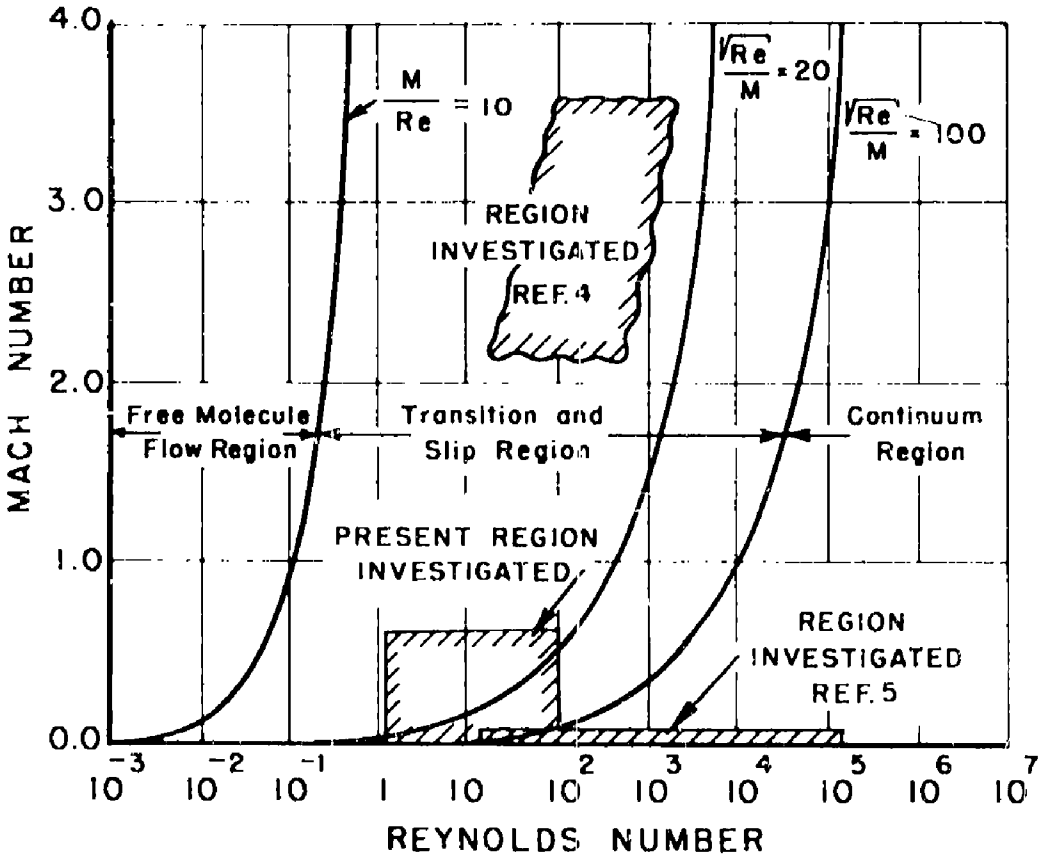


FIG. 1 - INVESTIGATED FLOW REGION

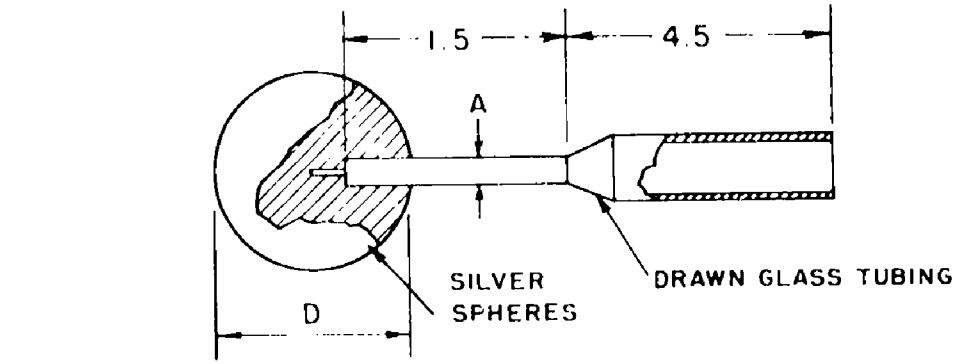


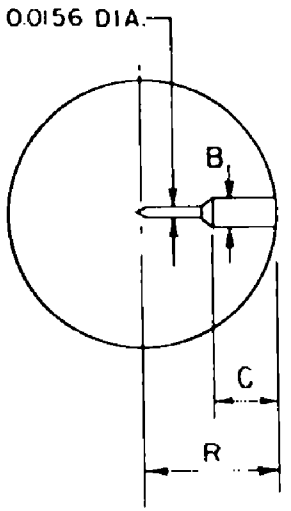


| D (IN.) | R (IN.) | A (IN.) | B (IN.) | C (IN.) |
|---|---|---|---|---|
| 0.10 | 0.050 | 0.010 | 0.015 | 0.025 |
| 0.175 | 0.0875 | 0.0175 | 0.022 | 0.0436 |
| 0.25 | 0.125 | 0.025 | 0.030 | 0.063 |
| 0.50 | 0.250 | 0.050 | 0.055 | 0.125 |

FIG.2-DIMENSIONS OF HEAT TRANSFER SPHERES

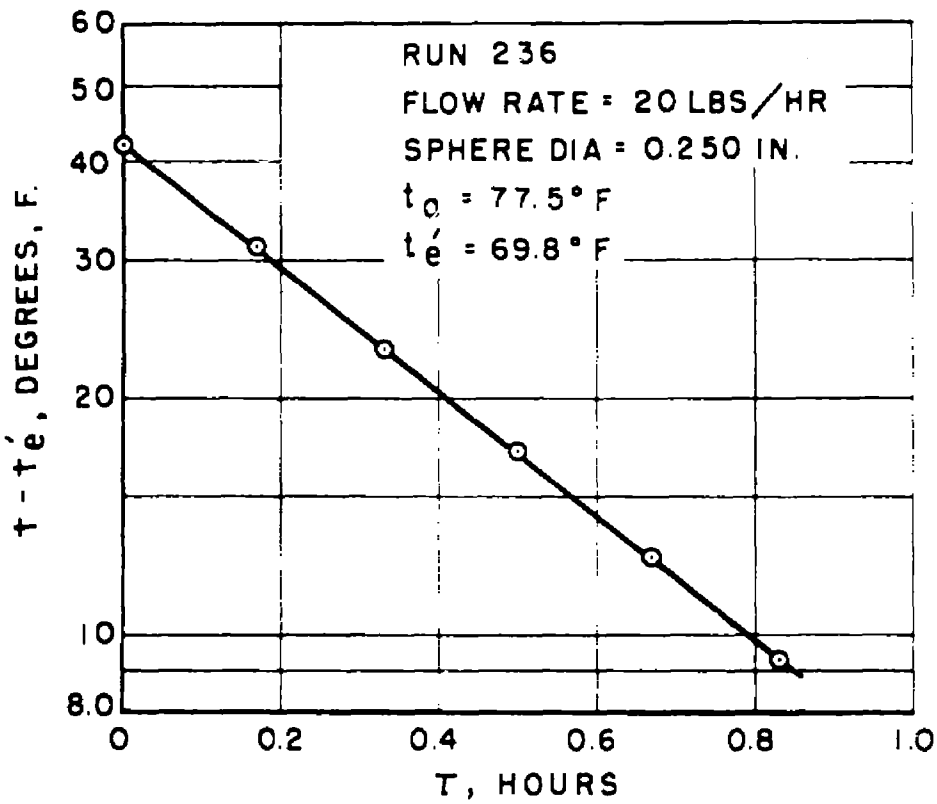


FIG. 3 – TYPICAL PLOT OF SPHERE TEMPERATURE WITH TIME

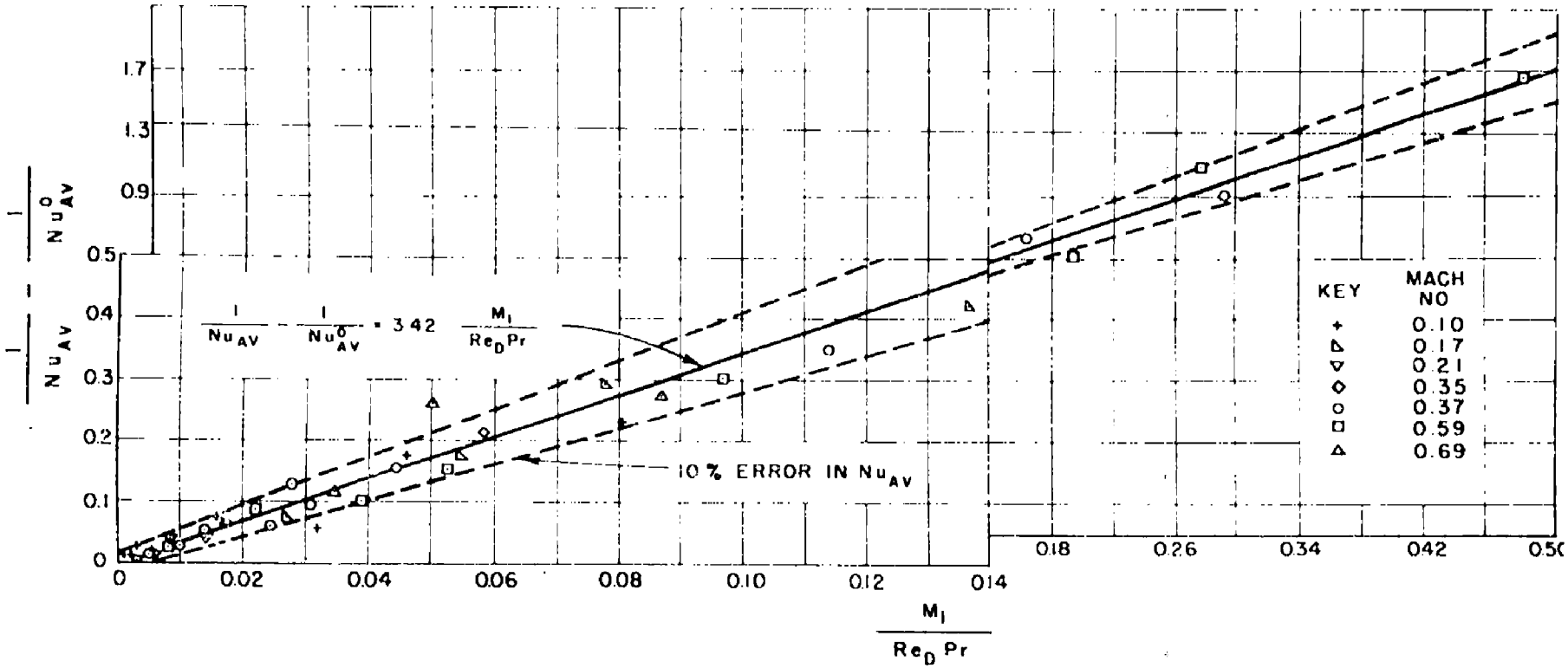


FIG. 4 - CORRELATION OF HEAT TRANSFER FROM SPHERES IN A RAREFIED SUBSONIC AIR STREAM

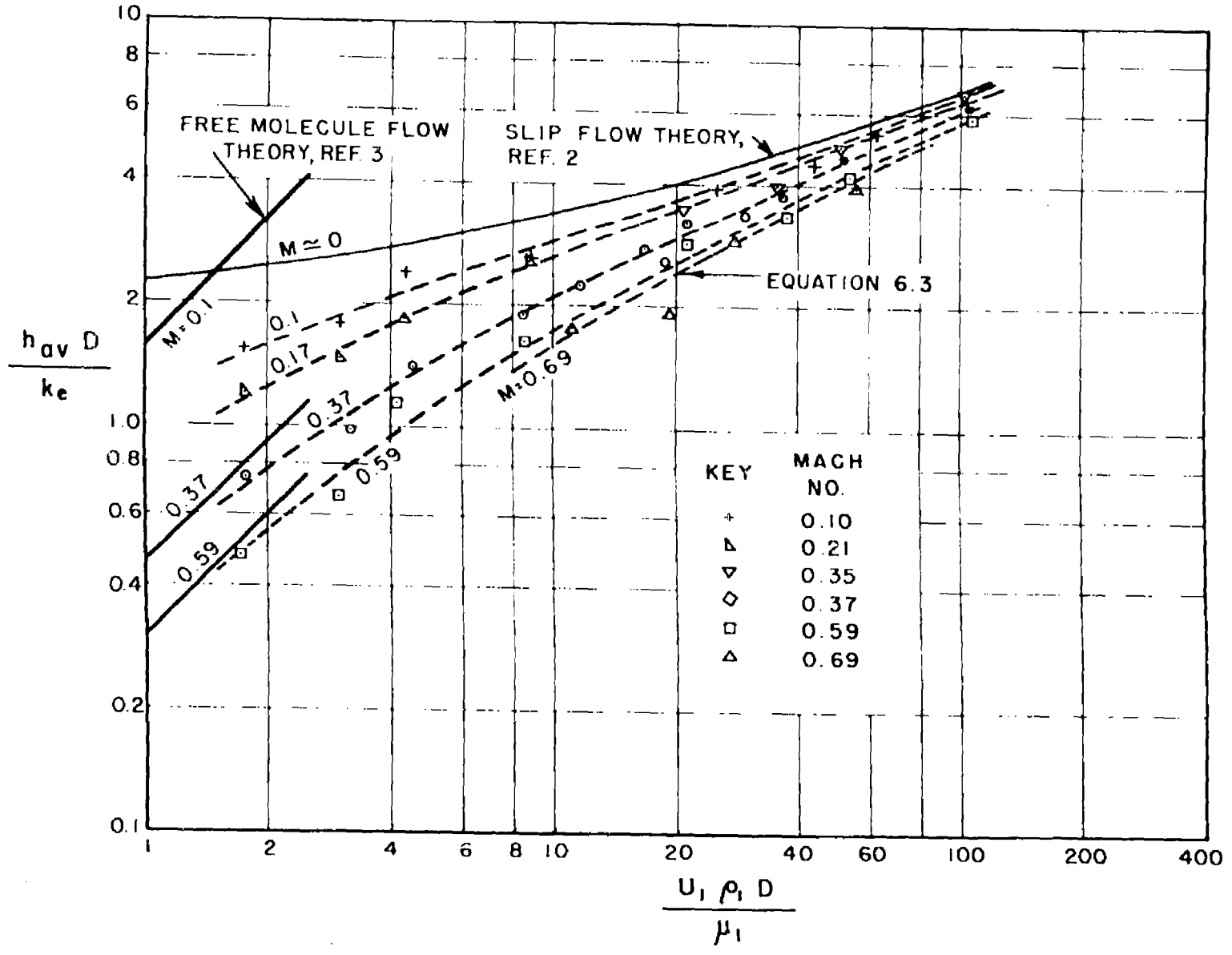


FIG. 5-AVERAGE HEAT TRANSFER COEFFICIENTS FOR SPHERES IN SUBSONIC FLOW TO RAREFIED AIR

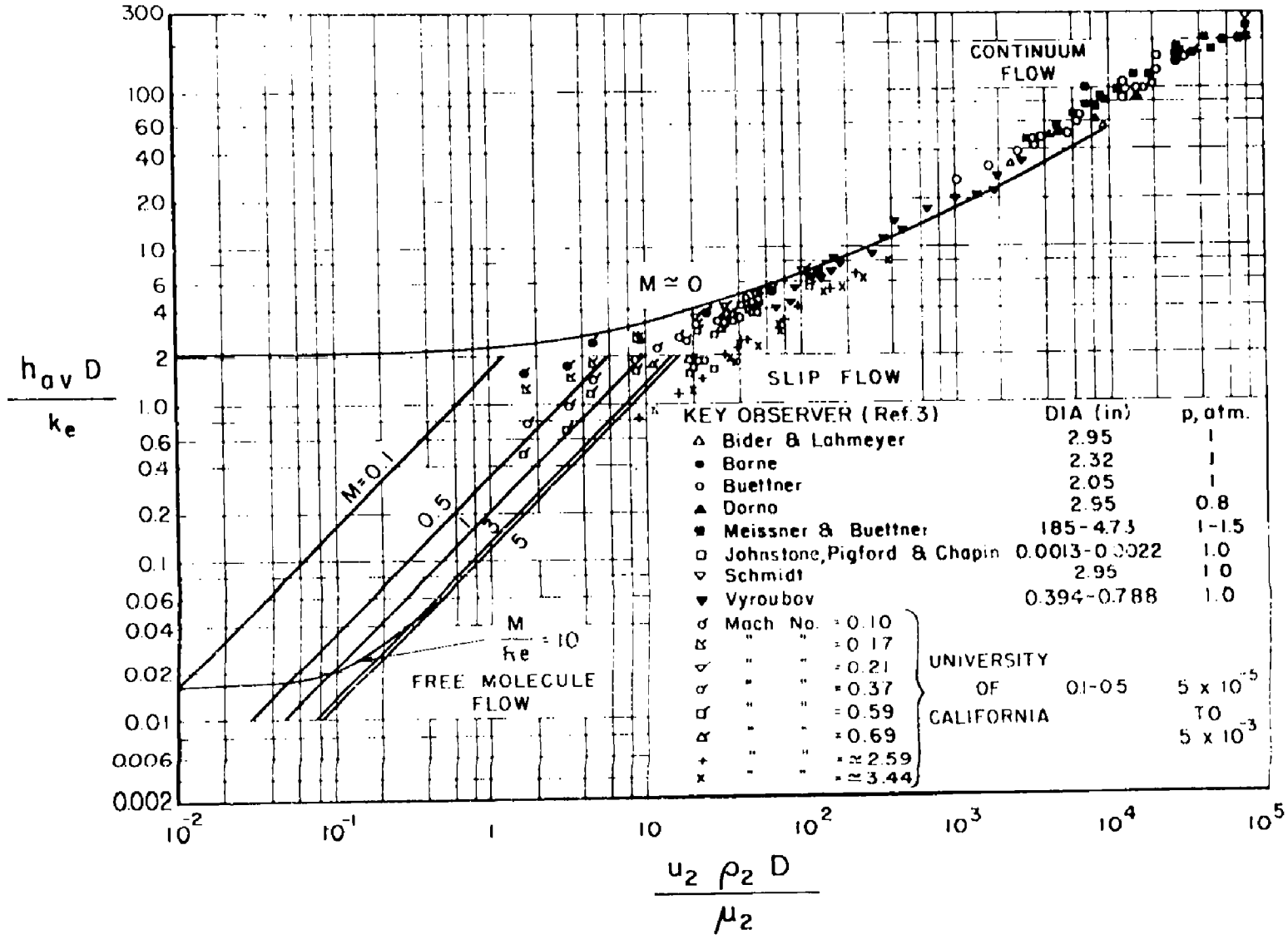


FIG. 6 – AVERAGE HEAT TRANSFER COEFFICIENTS FOR SPHERES IN AIR

UNCLASSIFIED